



## Turing Patterns in CNN's Based on a New Cell

Liviu Goras\* and Leon O. Chua\*\*

- \* Technical University Iași, Faculty of Electronics and Telecommunications, Bd. Copou 11, Iași 6600, Romania, tel/fax 4 032 211 667, e-mail lgoras@tuiasi.ro
- \*\* University of California at Berkeley, Nonlinear Electronics Laboratory, 258M Cory Hall, Berkeley, CA 94720 USA, tel (510) 642 5311, fax (510) 643 8869

**ABSTRACT** A new cell is proposed for CNN's able to produce Turing patterns. The conditions for generating Turing patterns in terms of the cell parameters are derived and several computer simulations are presented.

### 1. Introduction

The two-grid coupled Cellular Neural Networks (CNN's) architecture [1-5] has been recently shown to be capable to produce Turing patterns on the basis of a mechanism similar to that proposed by Turing [6],[7]. Composed of identical cells identically coupled by means of two homogeneous resistive grids, such CNN's exhibit an **unstable** homogeneous equilibrium point which corresponds to a **stable** one for an isolated cell. The pattern is one of the stable equilibrium points towards which the network emerges. The equations governing the dynamics of the array have the form:

$$\begin{aligned} \frac{du_y(t)}{dt} &= \gamma f(u_y, v_y) + D_u \nabla^2 u_y \\ \frac{dv_y(t)}{dt} &= \gamma g(u_y, v_y) + D_v \nabla^2 v_y \end{aligned} \quad (1)$$

where  $f(u, v)$  and  $g(u, v)$  are related to the two-port nonlinear resistive characteristics as shown in the next section,  $D_u$  and  $D_v$  the diffusion coefficients and  $\nabla^2$  is the discrete Laplacian. The so-called Turing conditions [5-7]

$$\begin{aligned} f_u + g_v &< 0 \\ f_u g_v - f_v g_u &> 0 \\ D_v f_u + D_u g_v &> 0 \\ (D_v f_u - D_u g_v)^2 + 4 D_u D_v f_v g_u &> 0 \end{aligned} \quad (2)$$

where  $f_u, f_v, g_u, g_v$  are elements of the Jacobian matrix of  $f(u, v)$  and  $g(u, v)$  have been shown [9] to be only necessary for discrete arrays. Obviously  $f_u$  and  $g_v$  as well as  $f_v$  and  $g_u$  should have opposite signs. The study performed in [8-11] considered CNN's based on the (reduced) Chua's circuit which, as a concrete vehicle to introduce the basics concepts, showed once again its capability of generating new exciting behaviors. In this case, using appropriate coupling resistors,  $f_u, g_u$  are positive and  $f_v, g_v$  negative. The aim of this communication is to investigate Turing patterns produced in CNN's based on another active cell for which  $f_u, f_v$  are positive and  $g_u, g_v$  negative.

### 2. The Cell

The two-port nonlinear dynamic cell shown in Fig.1 is proposed as the basic cell for CNN realization. It consists of four linear elements including a voltage controlled current source and a Chua's diode. The relations between parameters of the cell and those appearing in the overall equations are:

$$\gamma = \frac{1}{C_u}; D_u = \frac{G_u}{C_u}; D_v = \frac{G_v}{C_v}; g(u, v_i) = \frac{C_u}{C_v} \tilde{g}(u_i, v_i) \quad (3)$$

where  $i_u = f(u, v_i)$  and  $i_{2i} = \tilde{g}(u_i, v_i)$  are the equations describing the resistive part of the cell.

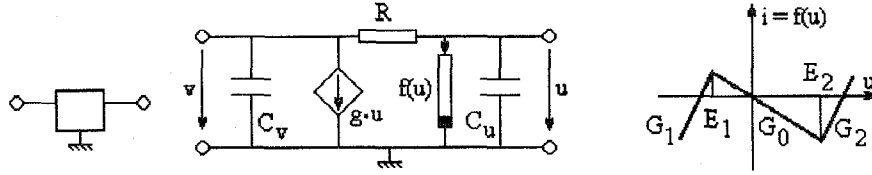


Figure 1: The new cell and the  $v$ - $i$  characteristic of the Chua's diode

Explicitly, the above algebraic functions are:

$$\begin{aligned} i_1 &= -Gu - f(u) + Gv \\ i_2 &= (G - g)u - Gv \end{aligned} \quad (4)$$

For the characteristic of the nonlinear resistor shown in Fig.1 the relations between the elements of the Jacobian matrix,  $\gamma$ ,  $D_u$ ,  $D_v$  and the parameters of the array are:

$$\begin{aligned} f_u &= -(G + G_0) & G &= f_v \\ f_v &= G & G_0 &= -(f_u + f_v) \\ g_u &= \frac{C_u}{C_v}(G - g) & \tilde{g} &= G - \frac{C_u}{C_v}g_u \\ g_v &= -\frac{C_u}{C_v}G & G_v &= C_v D_v \\ D_u &= \frac{G_u}{C_u} & C_u &= \frac{1}{\gamma} \\ D_v &= \frac{G_v}{C_{uv}} & C_v &= -C_u \frac{f_v}{g_v} \\ \gamma &= \frac{1}{C_u} & G_u &= \frac{D_u}{\gamma} \end{aligned} \quad (5)$$

Observe that there are seven degrees of freedom; i.e., the four elements of the Jacobian matrix and  $\gamma$ ,  $D_u$ ,  $D_v$  thus being possible to synthesize CNN's having any desired parameters.

### 3. Qualitative Explanation of Reaction-Diffusion Phenomena in a 1D CNN Based on the New Cell

We consider the array shown in Fig.2 and assume that the diffusion coefficients  $D_u$  and  $D_v$  of the  $u$ - and  $v$ -grid respectively satisfy the relation  $D_u \ll D_v$ ; i.e.,  $R_u C_u \gg R_v C_v$ . Suppose that the initial conditions are zero except for the voltage  $u_i$  which slightly increases. Due to the negative slopes of the nonlinear resistors for small voltages which determine the instability of the array, the voltage will continue to increase. Through the  $R_u$  resistors the increase of  $u_i$  will slowly "diffuse" to the neighboring cells on the  $u$ -part. As a consequence the neighboring cells will have their  $u$ - voltages increased in the vicinity of the  $i$  cell (local activation). At the same time, the voltage controlled source will determine the voltage of the opposite  $v$ -node decrease; i.e., become negative, and, due to the much smaller value of the time constant of the  $v$  grid, the negative voltage of the  $v_i$  node will propagate quickly on the  $v$ - side of the array (local activation

again). Thus, at a greater distance of the cell  $i$ , the negative voltage on the  $v$ - side of the array will determine, through the transversal resistors, the decrease of the opposite  $u$ - voltages (which were not able to increase as a consequence of the slow propagation of the initial perturbation on the  $u$ - side); i.e., a distance inhibition.

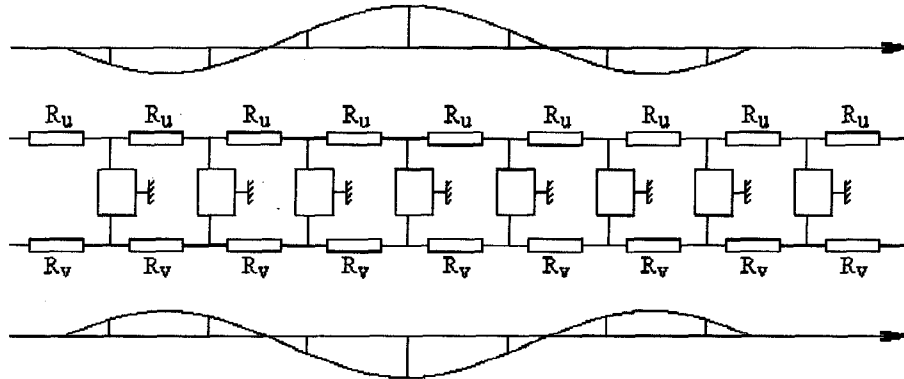


Figure 2: 1D array exhibiting reaction-diffusion Turing pattern behavior.

This way of reasoning can be applied for other points in the array as well; the voltages on the two sides of the array will grow up and down until the nonlinearity will bound them at various levels. The voltage levels on the two sides of the array are sketched in Fig.2 as well. Obviously, the spatial wavelengths will be determined among other parameters by the ratios between the diffusion coefficients.

The simulation results shown in Fig.3 confirm the above intuitive explanation. Similar consideration can be made for 2D arrays.

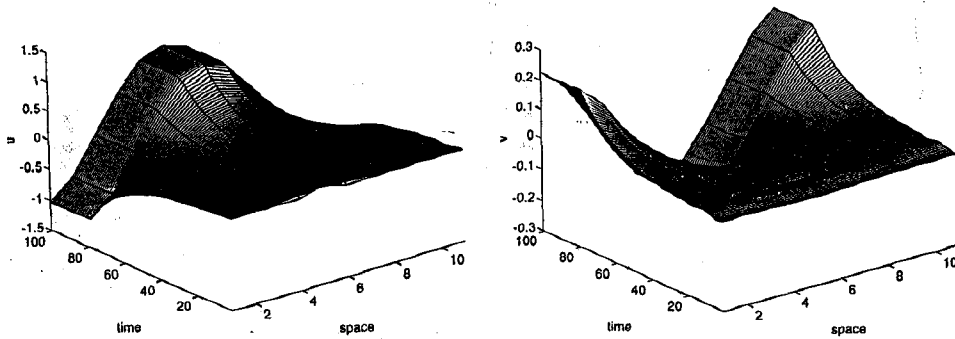


Figure 3: Simulated behavior of the time-space dynamics of the  $u$ - and  $v$ - voltages in a 11-cell 1D array starting from zero state except for the  $u$ - voltage of the 5th cell showing the validity of the intuitive explanation of the pattern formation mechanism.

**4. Simulation Results**

Qualitatively, the behavior of CNN's based on the proposed cell differs from that reported in [8-11] by the fact that the  $v$ - voltages are "opposite phase" with respect to the  $u$ - ones. In the following we present several simulation results for 1D and 2D arrays to show how patterns may be controlled, to a certain extent, by means of appropriate initial conditions. We emphasize the fact that, while for the 1D case, the mode selection has been successful for all simulations, in the 2D case the prediction of the final pattern has been sometimes unsuccessful as the nonlinearity has a role which is not yet enough understood.

We give below several examples of mode selection through initial conditions for the 1D and 2-D cases. In the 1D case we used a 50 cell 1D CNN with the parameters  $f_u=0.4$ ,  $f_v=1$ ,  $g_u=-0.25$ ,  $g_v=-0.5$ ,  $\gamma=28.2714$ ,  $D_u=1$ ,  $D_v=4$ . The band of unstable modes  $(0.11492, 0.43508)$  contained five spatial modes  $k_6^2=0.14045\dots k_{10}^2=0.38197$ . Using the initial conditions  $u_i(0)=0.1\cos[(2i+1)m\pi/100]$ ;  $v_i(0)=0$ , for  $m=6$  and  $m=10$  respectively and zero-flux boundary conditions, the dynamics shown in Fig.4 have been obtained.

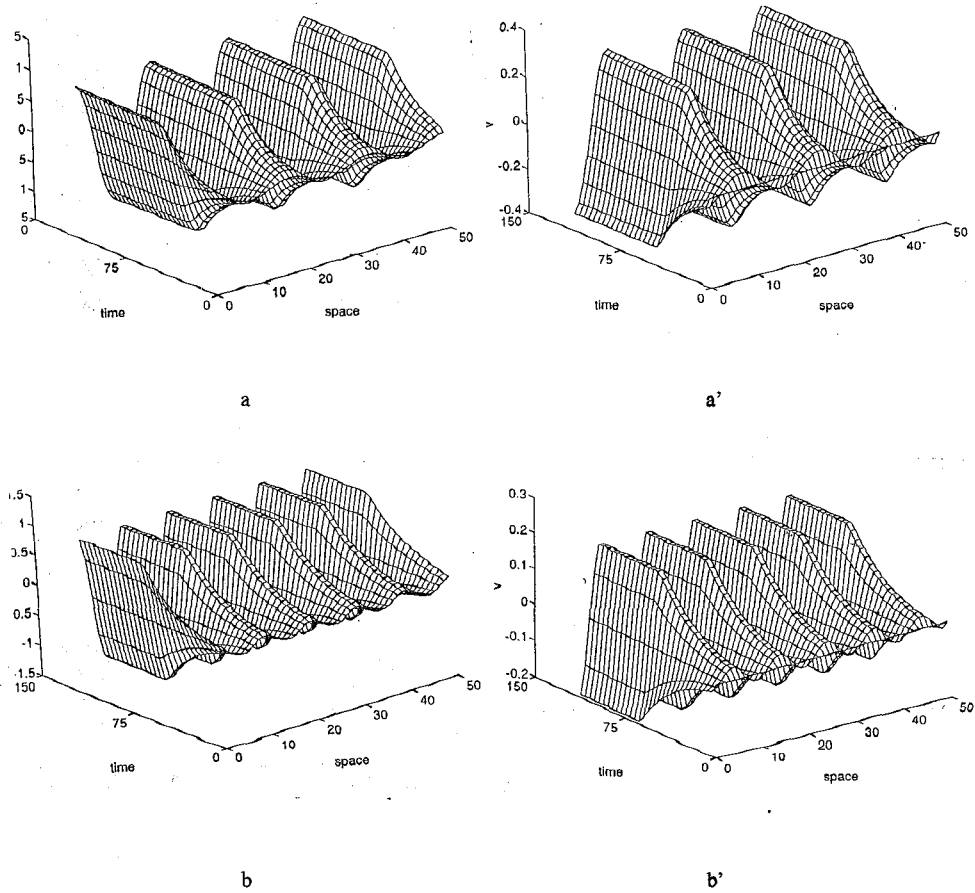


Figure 4: Time evolution of  $u$ - and  $v$ - variables in a 1D 50 cell CNN controlled through initial conditions, the modes 6 (a, a') and 10 (b, b') being excited.

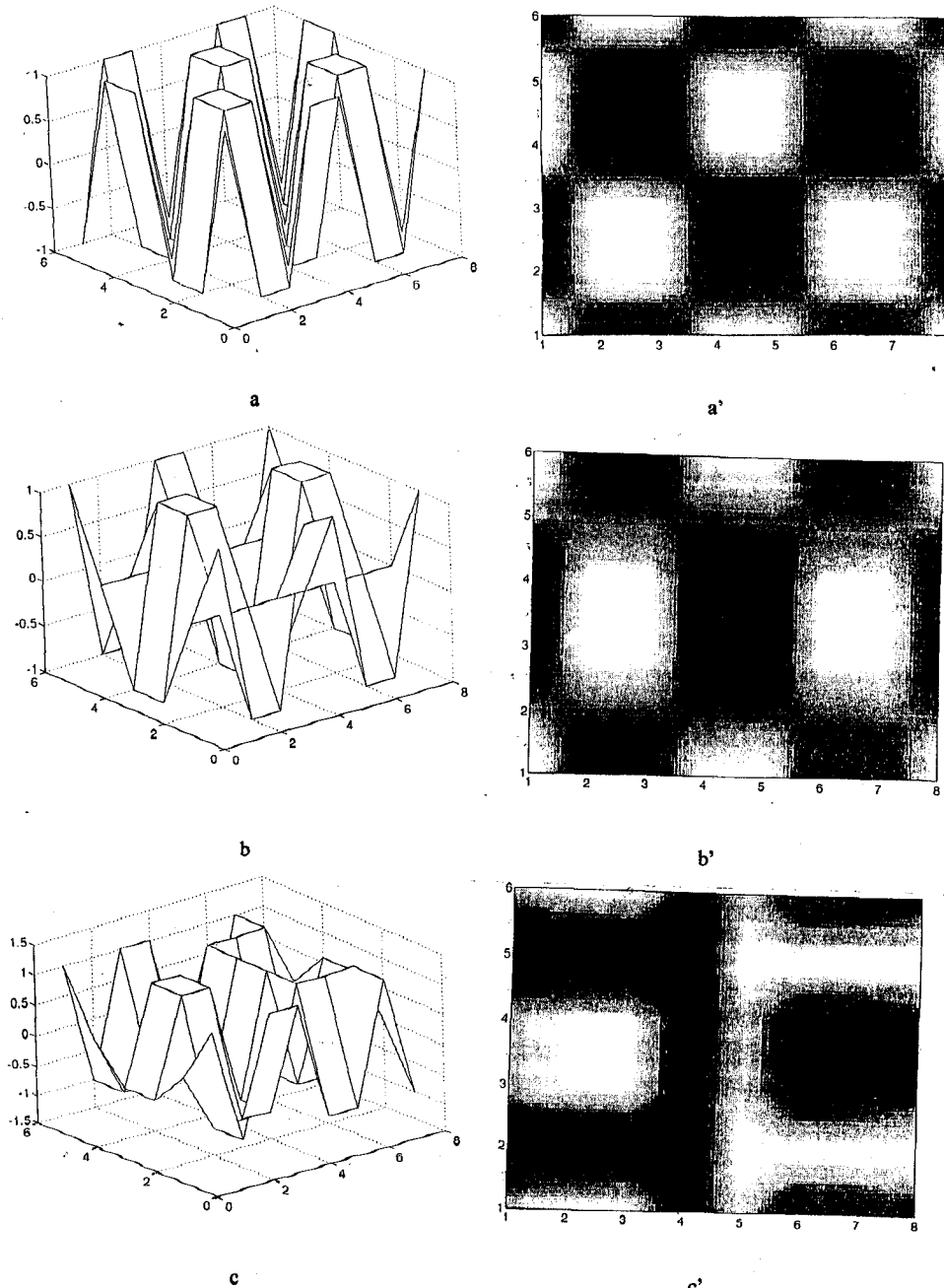


Figure 5: Final 2D patterns for successful [a, a' - mode (2,4), b, b' - mode (3,4)] and unsuccessful [c, c' - attempt to excite mode (4,1)] control through initial conditions.

In the 2D case we used an array of  $6 \times 8$  cells with the same parameters except for  $\gamma=28.40909$  and  $D_v=3.4$  corresponding to a band of unstable modes (2.58893...4.59096) with 23 modes inside. Using zero-flux boundary conditions and initial conditions of the form  $u_{ij}(0)=0.5\cos[(2i+1)m\pi/12] \times \cos[(2j+1)n\pi/16]$  and  $v_{ij}(0)=0$  we obtained for  $(m=2, n=4)$ ,  $(m=3, n=4)$  and  $(m=4, n=1)$  the results presented in Fig.5. From the last image one sees that the obtained pattern has little resemblance to that expected from linear theory: the  $(4,1)$  mode led to an unstable pattern that evolved to another one, stable but different.

### 5. Concluding Remarks

The new cell proposed for CNN's capable to produce Turing patterns has been shown to allow designing CNN's with any desired parameters. Pattern control using initial conditions can be realized even patterns different to those predicted by linear theory are possible as well.

**Acknowledgments** This research has been accomplished at the Nonlinear Electronics Laboratory, University of California at Berkeley, with gratefully acknowledged financial support from the Fulbright Foundation.

### References

- [1] L. O. Chua, L. Yang, "Cellular Neural Networks: Theory", IEEE Trans. Circuits Syst., vol. 35, no 10, pp. 1257-1272, October 1988.
- [2] L. O. Chua, L. Yang, "Cellular Neural Networks: Applications", IEEE Trans. Circuits Syst., vol. 35, no 10, pp 1273-1290, October 1988.
- [3] T. Roska, J. Vanderwalle, Cellular Neural Networks, John Wiley & Sons, 1993.
- [4] A. Rodriguez Vazquez, S. Espejo and R. D. Castro, "VLSI Implementation of the analogic CNN Universal Machine Including On-Chip Photosensors", in B. Sheu, M. Ismail, E. S. Sinencio, T. H. Wu (Editors) Microsystem Technology for Multimedia Applications: An Introduction, IEEE Press, 1995.
- [5] A. M. Turing, "The Chemical Basis of Morphogenesis", Phil. Trans. Roy. Soc. Lond. B 237, pp.37-72, October 1952.
- [6] J. D. Murray, Mathematical Biology, Springer-Verlag, Berlin Heidelberg, 1993.
- [7] V. P. Munuzuri, M. G. Gesteira, A. P. Munuzuri, L. O. Chua, V. P. Villar, "Sidewall Forcing of Hexagonal Turing Patterns: Rhombic Patterns", Memorandum No. UCB/ERL M94/35, April 1994.
- [8] L. Goras, L. O. Chua, D. M. W. Leenaerts, "Turing Patterns in CNN's-Part I: Once Over Lightly", IEEE Trans. Circuits Syst, vol.42, pp. 602-611, October 1995.
- [9] L. Goras, L. O. Chua, "Turing Patterns in CNN's - Part II: Equations and Behaviors", IEEE Trans. Circuits Syst, vol.42, pp. 612-626, October 1995.
- [10] L. Goras, L. O. Chua, L. Pivka, "Turing Patterns in CNN's - Part III: Computer Simulation Results", IEEE Trans. Circuits Syst, vol.42, pp. 627-636, October 1995.
- [11] D. M. W. Leenaerts, L. Goras, L. O. Chua, "On the Properties of Turing Patterns in a Two-Cell CNN", Proceedings of the International Symposium on Signals, Circuits and Systems, SCS'95, Iasi, 19-21 October 1995.